Fatty acid synthase (FASN), a novel signature for visceral adipose tissues, regulates proliferation, migration and predicts prognosis of clear cell renal cell carcinoma

Wen-Hao Xu
Fudan University Shanghai Cancer Center https://orcid.org/0000-0002-0660-9162
Aihetaimujiang Anwaier
Department of Urology
Hong-Kai Wang
Department of Urology
Jun Wang
Department of Urology
Wen-Kai Zhu
Department of Urology
Xi Tian
Department of Urology
Chung-Guang Ma
Department of Urology
Fang-Ning Wan
Department of Urology
Da-Long Cao
Department of Urology
Guo-Hai Shi
Department of Urology
Yuan-Yuan Qu
Department of Urology
Hai-Liang Zhang
Department of Urology
Ding-Wei Ye (2406841044@qq.com)
Department of Urology https://orcid.org/0000-0002-6761-5195

Research

Keywords: FASN, visceral adipose tissue, body mass index, clear cell renal cell carcinoma, prognosis

Posted Date: February 24th, 2020

DOI: https://doi.org/10.21203/rs.2.24247/v1

Abstract

Background: Growing evidence has indicated obesity one of the important etiological indicators of clear cell renal cell carcinoma (ccRCC). This study aims to investigated FASN mRNA expression in anthropometric adipose tissue, and elucidate prognostic value and potential functions in ccRCC patients.

Methods: Transcriptional expression profiles was obtained from 380 paired ccRCC and adjacent normal tissues from Fudan University Shanghai Cancer Center (FUSCC) and 533 ccRCC samples from the Cancer Genome Atlas (TCGA) cohort. The visceral adipose tissue (VAT) and the subcutaneous adipose tissue (SAT) at the level of the umbilicus were measured using magnetic resonance imaging. The Kaplan-Meier method and log-rank test, with cooperation from Cox regression analysis, were used in survival analysis. Subsequently, we transiently transfected FASN plasmid into A498 and 786O cells, and investigated the role of FASN in ccRCC cell proliferation, apoptosis and migration in vitro. Related hub gens, functional annotations and significant signal pathways were predicted using integrated bioinformatics.

Results: FASN mRNA expression was significantly higher in tumor than normal tissues in 913 ccRCC patients from FUSCC and TCGA cohorts. In addition, increased FASN mRNA expression was significantly relevant to advanced T stage ($p < 0.001$), N stage ($p = 0.019$), and AJCC stage ($p = 0.002$). Pearson's correlation coefficient indicated that FASN amplification positively correlated with VAT% ($r = 0.772$, $p < 0.001$). VAT% was significantly correlated with poor PFS and OS, with hazard ratios of 2.066 (1.113-7.261, $p = 0.028$) and 2.773 (1.168-8.974, $p = 0.023$) in FUSCC. Meanwhile, ccRCC patients with elevated FASN expression significantly responded for poor PFS and OS, with hazard ratios of 1.529 (1.135-2.061, $p = 0.005$) and 1.450 (1.030-2.041, $p = 0.033$). Next, after transfection efficiency was verified in A498 and 786O cells, we found transient inhibition and overexpression of FASN significantly regulates cells proliferation and migration abilities, and inhibition of FASN displayed higher apoptotic rate in ccRCC cells.

Conclusion: In conclusion, this study demonstrated that FASN mRNA expression is positively related with aggressive proliferation, migration progression and predicts prognosis of ccRCC. In addition, we first reveal that elevated FASN mRNA expression is significantly correlated with abdominal obesity distribution, especially VAT%, which also is a significant predictor of poor prognosis in patients with ccRCC.

Background

Renal cell carcinoma (RCC) is a highly malignant tumors originating from the urinary tubular epithelial system of the renal parenchyma, and incidence of RCC is increasing at a rate of 2% a year, especially in developed country [1]. Pathologically, RCC can be divided into four subtypes, and the vast majority of which is clear cell renal cell carcinoma (ccRCC), accounting for approximately 70% of cases [2]. ccRCC portends highly aggression and poor prognosis even in patients who were diagnosed in early stage and

treated with nephrectomy [3, 4]. Contemporarily, many indicators of poor prognosis contributing to RCC have been confirmed, including obesity and physical inactivity.

Fatty acid synthase (FASN) is one of the important enzymes involved in lipid metabolism. FASN uses NADPH (reduced nicotinamide adenine dinucleotide phosphate) as a reductant, acetyl-CoA as a primer and malonyl-CoA as a substrate to synthesize long-chain fatty acids [5]. But in well-nourished individuals, most of the fatty acids are provided by exogenous fatty acid from diet, which makes the role of FASN less important [6]. FASN is low expressed in most normal cells and tissues, except for cycling endometrium and lactating breast in adults [7]. Compared with normal cells, all esterified fatty acids in most tumor cells are synthesized from scratch, and the expression of FASN in tumor cells is significantly increased, which is related to tumor aggression and poor prognosis in several cancer types. [5, 8, 9]. Notably, Hakimi et al. indicated that the upregulated expression of FASN was also significantly associated with poor prognosis[10]. Therefore, FASN may cause the tumorigenesis of ccRCC based on its lipid metabolism pathway.

Several studies indicated that obesity, defined as body mass index (BMI) greater than 30 kg/m², has been identified as a risk factor for ccRCC [11–13]. Whether ccRCC patients who received nephrectomy or metastatic ccRCC patients who had been treated with targeted therapy, obese patients survive longer than those with normal weight (BMI 18·5–24·9 kg/m², according to WHO's BMI categories) [14, 15]. However, there is a counterintuitive association between BMI and prognosis [16]. Although BMI is an internationally accepted convenient and effective weight indicator, recently, many researchers have controversies on the accuracy of BMI in indicating body fat distribution and metabolic risks [17–19]. So, it is essential to present a new measurement to indicate the distribution of adipose and its prognostic value in ccRCC [20, 21].

In 2010, Ibrahim MM indicated the anatomical, cellular, molecular difference of subcutaneous adipose tissue (SAT) and visceral adipose tissue (VAT), and described the heterogenous nature of obesity [22]. Unlike SAT (present in subcutaneous areas), VAT present around abdominal viscera in mesentery and omentum, and is associated with inflammation, type II diabetes and several fat-related diseases [22, 23]. Recent study also showed that ccRCC patients with higher Fuhrman grade contribute to significant correlation with elevated VAT [24]. How to more precisely indicate the distribution of adipose and which parts of adipose in body will affect the disease through which metabolic pathway has become the focus in recent study, especially in ccRCC.

To define the prognostic implications of FASN mRNA expression in ccRCC patients and the correlation of FASN mRNA and adipose, we recruited 533 ccRCC samples from TCGA cohort, and 380 patients who have received radical nephrectomy in our institution. Functional annotations of FASN and its involved signaling pathways have been conducted in vitro or in silico. In this study, we hypothesized that elevated FASN mRNA expression correlates with VAT%, poor prognosis and malignant biologic behaviors of ccRCC.

Materials And Methods

Patients and variables

A total of 380 ccRCC patients from the Department of Urology, Fudan University Shanghai Cancer Center (FUSCC, Shanghai, China) with available pathology reports and electronic medical records were consecutively enrolled in analyses from August 2009 to November 2018. This study also consecutively included 533 ccRCC patients with available RNA sequence data from the Cancer Genome Atlas (TCGA) database. Tissue samples, including ccRCC and adjacent normal tissue, were collected during surgery and fixed in 4% paraformaldehyde, available from FUSCC tissue bank. Clinicopathological parameters of all patients, including age at surgery, gender, Body Mass Index (BMI), tumor laterality, TNM stage, American Joint Committee on Cancer (AJCC) stage, International Society of Urological Pathology (ISUP) grade. Anthropometric measures of obesity on magnetic resonance imaging (MRI), including anterior abdominal adipose thickness (A in blue line), posterior abdominal adipose thickness (P in pink line), subcutaneous adipose tissue (SAT) and visceral adipose tissue (VAT), were collected and analyzed in this study.

Total mRNA extraction and Real-Time Quantitative PCR (RT-qPCR)

Total RNA sequence was isolated using TRIzol reagent (Invitrogen, Carlsbad, CA) from 380 paired ccRCC and adjacent normal samples or cells. SYBR® Premix Ex TaqTM (TaKaRa) was implemented to perform qRT-PCR reactions in triplicate according to attached protocols. The primers of FASN were forward: 5'-CGACAGCACCAGCTTCGCCA-3' and reverse: 5'- CACGCTGGCCTGCAGCTTCT-3'. The relative FASN expression quantity was measured after the $2^{-\Delta\Delta Ct}$ calculation using beta-Actin as the internal standard. Relative expression in this study was represented using the ratio of FASN expression in Tumor/Normal tissues (T/N).

Anthropometric measures of obesity

The quantity of anterior abdominal adipose thickness (A in blue line), posterior abdominal adipose thickness (P in yellow line) and anteroposterior diameter (AP in pink line) was measured by MRI at the umbilical level (approximately L4-L5 level marked in green dotted line) with T2-weighted sagittal localization images for 380 patients. The visceral obesity percentage was defined as VAT%. As previously described[25], the value of SAT and VAT% was calculated using the formula SAT = A + P and VAT%= [(AP-SAT)/AP], respectively.

Cell culture

Two normal types of human ccRCC cell lines (A498 and 786O) were obtained from American Type Culture Collection (ATCC). The A498 and 786O cells were cultured in culture medium RPMI-1640 (GIBCO, USA), supplemented with 10% fetal bovine serum (Hycline, Life Sciences, Shanghai, China) and 100 U/ml

penicillin (Beyotime, China). A498 and 786O cells were incubated in a humidified atmosphere incubator of 5% CO_2 at 37ºC temperature.

Cell transfection

Both A498 and 786O cells have been transfected with double stranded siRNA according to the manufactures' protocol using plasmid using Lipofectamine 2000 reagent (RiboBio). The normal control of A498 and 786O cells refers to control lentiviral vectors added in the infected cell suspension. A498 and 786O cells were harvested for at least 24 hours after transfection for further experimental analysis.

Protein isolation and Western blot analysis

Proteins were extracted from A498 and 786O cells using RIPA lysis buffer (Beyotime Biotechnology Shanghai, China), and concentrated by the bicinchoninic acid protein assay kit (Beyotime Biotechnology, Shanghai, China). Samples were separated by electrophoresis on 6% or 10% SDS gel and then transferred to a methanol activated polyvinylidene fluoride (PVDF) membrane. Membranes were blocked with 5% bovine serum albumin (5% BSA) for 1 h at room temperature and then incubated with primary antibodies, anti-FASN (1:1000, ab22759, Abcam), and anti-beta-Actin primary antibody (1:3000, ab179467, Abcam) at 4 °C overnight. After washed for with TBST for three times, membranes were incubated with secondary antibody Goat Anti-Rabbit IgG conjugated with HRP (1:3000, ab205718, Abcam) at room temperature for 60 min. After three washes with TBST for 10 min each, the bands were visualized using ECL-plus™ western blotting chemiluminescence kits (BD Biosciences, New Jersey, USA).

Cell viability analysis

For viability assays, cells treated with shRNAs or inhibitors were seeded onto 96-well plates (2,000 cells/well). Next, 10 μL CCK8 solution (KeyGEN BioTECH, Nanjing, Chian) was added to each well, and cells were incubated at 37 °C for 2 h. The absorbance of each well at 450 nm was measured at 1, 2, 3, 4, and 5 days after seeding using an automatic microplate reader (TEAN, Swiss). Three replicate analyses were performed for each sample.

Cell apoptosis assays

Apoptosis detection assay was performed using Annexin V-FITC Apoptosis Detection Kits (BD, USA) in accordance with the manufacturer's procedures. Briefly, A498 and 786O cells were obtained and triple washed with PBS, and then added 500 ul in 1 × binding buffer. 500 ul cell suspension, 5 ul Annexin V-FITC, and 5 ul propidium iodide (PI) solution were resuspended in each collection tube. After incubation for 15 min, cell apoptosis was analyzed using a FACS analyzer (BD, USA).

Transwell migration assay

After trypsinized and suspended in the medium, 1×10^5 A498 and 786O cells were seeded in medium with 10% FBS and placed in each Transwell chamber. The medium containing 20% fetal bovine serum was added in the lower 24-well plate chamber. After 24 hours, the bottom A498 and 786O cells were treated with 4% poly-oxymethylene for 15 minutes, deionized water, and 0.1% crystal violet for 30 minutes.

Finally, the A498 and 786O migrating to the lower surface of Transwell chamber were counted using a microscope in six random fields.

Survival analysis

Chi-squared test was utilized to find out the association between different FASN mRNA expression sets and categorical clinicopathological data distribution. Pearson's correlation coefficient was utilized to determine association between VAT% and levels of FASN mRNA expression.

The primary endpoint was overall survival (OS), which was assessed from the date of receive radical nephrectomy to the date of death or the last follow-up. Progression-free survival (PFS) was the secondary endpoint and was defined as the length of time from the date of surgery to the date of progression, second-line treatment or death, whichever accrued first. Survival curves were established using the Kaplan-Meier method and analyzed by log-rank test with 95% confidence intervals (95% CI). To find independent predictors, the hazard ratio (HR) estimates and 95% CI were performed using univariate and multivariate Cox logistic regression model. As a supplement to survival, Cox logistic regression analysis was performed on 117 patients with available MRI scan to assess confounding covariates including A, P, SAT, VAT%, TNM stage, ISUP grade and FASN expression.

Protein–protein interaction (PPI) network construction

Search Tool for the Retrieval of Interacting Genes (STRING; http://strin g-db.org) (version 10.0) online database was utilized to detect PPI network of co-regulated hub genes and analyze the functional interactions between relative proteins. An interaction with a specificity score high than 0.4 was regarded as statistically significant.

Functional annotations

Database for Annotation, Visualization and Integrated Discovery (DAVID; http://david.ncifcrf.gov; version 6.8) online database were utilized to investigate the gene ontology (GO): BP (biological process), GO: MF (molecular function) and KEGG pathways analyses, then visualized in bubble chart. To predict potential hallmarks, gene set enrichment analysis (GSEA) was utilized to test significant genes using transcriptional sequences in TCGA database. A permutation test with 1000 times was used to identify the significantly changed pathways. Adj. p (the adjusted p values) less than 0.01 and FDR (false discovery rate) less than 0.25 were confirmed as significant related genes.

Statistical analysis

All statistical analyses and graphical plotting were performed with SPSS version 23.0 software or R software (version 3.3.2). All hypothetical tests were two-sided and p-values less than 0.05 were considered significant in all tests.

Results

In this study, research was conducted in three phases. First, significant differential FASN mRNA expressions and its novel implications in prognosis for 913 ccRCC patients from TCGA and FUSCC were assessed. Second, relationship among visceral adipose tissue, FASN expression, and prognosis for 117 ccRCC patients from FUSCC cohort was estimated. Third, effective experiments of FASN in human ccRCC cells were performed in vitro. Significant hub genes panel, functional annotations and signal pathways has been predicted using integrated bioinformatics methods.

Differential FASN mRNA expression and its correlation with advanced clinicopathological parameters in ccRCC patients from TCGA cohort

To explore the potential relationship between FASN expression and clinicopathological features of ccRCC patients, we enrolled 533 ccRCC samples and 72 adjacent normal samples from TCGA cohort, and found significantly increased FASN mRNA expression in ccRCC samples ($p < 0.05$; Fig. 1A). Additionally, the FASN mRNA expression was markedly related with advanced clinical AJCC stage ($p < 0.05$), and reached the highest in stage 4 (Fig. 1B). Kaplan-Meier method showed that elevated FASN expression was significantly associated with shorter PFS ($p = 0.011$) and OS ($p < 0.001$) in TCGA cohort (Fig. 1C-D). Overall, elevated FASN mRNA expression was significantly correlated with advanced clinicopathological features and poor prognosis in ccRCC patients based on TCGA cohort.

Clinicopathological characteristics of FUSCC cohort

Additionally, 380 ccRCC patients with paired available tumor and normal samples were enrolled from FUSCC cohort. Clinicopathological characteristics baseline of 380 patients in relation to FASN expression status was shown in Table 1. Chi-square test showed that baseline data were balanced on the distribution of categorical data. Increased FASN mRNA expression in ccRCC patients significantly correlated with advanced T stage ($p < 0.001$), N stage ($p = 0.019$), and AJCC stage ($p = 0.002$) in the FUSCC cohort.

Table 1

Clinicopathological characteristics in relation to FASN expression status in 380 ccRCC patients from FUSCC cohort.

Variable	Entire group (n = 380)	FASN mRNA expression		χ^2	P value
		Low expression (n = 190)	High expression (n = 190)		
Age at surgery (y, median ± SD)		54.1 ± 12.2	56.2 ± 11.4		
BMI (kg/m^2, median ± SD)		24.5 ± 3.3	23.5 ± 8.3		
Sex (n, %)				0.012	0.914
Male	249 (65.5)	125 (65.8)	124 (65.3)		
Female	131 (34.5)	65 (34.2)	66 (34.7)		
Laterality (n, %)				0.168	0.682
Left	190 (50.0)	97 (51.1)	93 (48.9)		
Right	190 (50.0)	93 (48.9)	97 (51.1)		
T stage at presentation (n, %)				16.645	< 0.001
T1-T2	309 (81.3)	170 (89.5)	139 (73.2)		
T3-T4	71 (18.7)	20 (10.5)	51 (26.8)		
N stage at presentation (n, %)				5.463	0.019
N0	333 (87.6)	174 (91.6)	159 (83.7)		
N1	47 (12.4)	16 (8.4)	31 (16.3)		
M stage at presentation (n, %)				2.522	0.112
M0	310 (81.6)	161 (84.7)	149 (78.4)		
M1	70 (18.4)	29 (15.3)	41 (21.6)		
AJCC stage				9.997	0.002

ccRCC, clear cell renal cell carcinoma; FUSCC, Fudan University Shanghai Cancer Center; BMI, body mass index; AJCC, American Joint Committee on Cancer; MRI, magnetic resonance imaging; SAT, subcutaneous adipose tissue; VAT, visceral adipose tissue

*P value less than 0.05 was considered as statistically significance, and marked in bold.

Variable	Entire group (n = 380)	FASN mRNA expression		χ^2	P value
		Low expression (n = 190)	High expression (n = 190)		
I-II	292 (76.8)	159 (83.7)	133 (70.0)		
III-IV	88 (23.2)	31 (16.3)	57 (30.0)		
ISUP grade (n, %)				0.675	0.411
1–2	182 (47.9)	95 (50.0)	87 (45.8)		
3–4	192 (52.1)	95 (50.0)	103 (54.2)		
ccRCC, clear cell renal cell carcinoma; FUSCC, Fudan University Shanghai Cancer Center; BMI, body mass index; AJCC, American Joint Committee on Cancer; MRI, magnetic resonance imaging; SAT, subcutaneous adipose tissue; VAT, visceral adipose tissue					
*P value less than 0.05 was considered as statistically significance, and marked in bold.					

Validation of increased *FASN* expression in ccRCC tissues from FUSCC cohort

In order to validate *FASN* mRNA expression levels in ccRCC tissues in vitro, we performed Real-time qPCR on 380 pairs of ccRCC and normal samples from FUSCC cohort. The result showed that the ratio of T/N was dramatically different among the distinct of *FASN* mRNA expression group (Figure 2A; 5.6% in T/N≤1, 48.3% in 1<T/N≤2, 29% in 2<T/N≤4, 13% in 4<T/N≤8, 2.6% in 8<T/N). Survival analysis demonstrated that patients with higher *FASN* mRNA expression exhibited significantly poor PFS (p<0.001; Figure 2B) and OS (p <0.001; Figure 2C). For relative low *FASN* expression patients, the median PFS was 65 months and the median OS was 71.5 months, respectively. For relative high *FASN* expression patients, the median PFS was 41 months and median OS was 65 months.

Cox regression analyses of FUSCC cohort.

Univariate and multivariate Cox regression analysis was performed in 380 ccRCC patients from FUSCC cohort. In univariate Cox regression analysis (Supplementary Table 1), recognized predictors such as TNM stage, ISUP grade, AJCC stage markedly correlated with PFS (p<0.001) and OS (p<0.001). Besides, age at surgery and BMI were also significantly related to PFS (p=0.024, p=0.017) and OS (p=0.021, p=0.012). Importantly, elevated *FASN* expression was significantly associated with poor PFS (HR=1.854, p<0.001) and OS (HR=2.017, p<0.001) in 380 ccRCC patients from FUSCC cohort.

In multivariate Cox regression analysis, pN stage, pM stage, ISUP grade and AJCC stage were still relevant to both PFS (pN stage: p=0.004, pM stage: p=0.011, ISUP grade: p<0.001, AJCC stage: p=0.002)

and OS (pN stage: p=0.009, pM stage: p=0.006, ISUP grade: p=0.002, AJCC stage: p<0.001). Importantly, elevated *FASN* expression was significantly correlated with poor PFS (HR=1.529, p=0.005) and OS (HR=1.450, p=0.033) in patients from FUSCC cohort, displayed in forest plots (Figure 2D-E).

VAT% is a more accurate obesity indicator for ccRCC

To verify the VAT% a better predictor using MRI scanning than BMI (Figure 3A), we detected correlations between VAT, BMI and *FASN* mRNA expression. Pearson's correlation coefficient suggested that elevated *FASN* mRNA expression was positively correlated with the VAT% (y=1.18x + 71.36, r=0.722, p<0.0001; Figure 3B). Additionally, we assessed BMI level in ccRCC patients from FUSCC cohort. The results showed that the BMI level in low *FASN* expression patients was significantly higher than that of patients with high *FASN* expression (p=0.0146; Figure 3C).

Univariate Cox analysis indicated that SAT, VAT%, TNM stage, ISUP grade and *FASN* expression are independent parameters for prognosis of 117 ccRCC patients (Supplementary Table 2). In multivariate Cox regression analyses of PFS and OS in 117 ccRCC cases whose MRI scans were available from FUSCC cohort, high VAT% was significantly associated with poor PFS (HR=2.066, p=0.028; Figure 3D) and OS (HR=2.773, p=0.023; Figure 3E). However, BMI was not independent covariate affecting survival. In addition, advanced pT (HR=1.132, p=0.037), pN (HR=10.63, p<0.001), pM (HR=17.72, p<0.001) and *FASN* expression (HR=2.578, P=0.008) was significantly correlated with poorer PFS (Figure 3D). SAT (HR=0.955, p=0.045), advanced pT (HR=2.526, p=0.014), pN (HR=12.23, p<0.001), pM (HR=13.736, p<0.001) and FASN expression (HR=2.33, p=0.003) was also markedly related with poor OS in 117 ccRCC cases (Figure 3E).

FASN regulates proliferation of ccRCC cells

Metabolism reprogramming is a hallmark of cancer and is vital in the progression of ccRCC cancer. We investigated *FASN* expression level in A498 and 786O cells after transfection with normal control, *FASN*-RNAi1, *FASN*-RNAi2 and *FASN*-overexpression (OE) plasmid, and cell viability and cell apoptosis were measured. It demonstrated that the *FASN* protein and mRNA expression significantly decreased in the *FASN* RNAi-transfecting cells, whereas increased in the *FASN* OE-transfecting group in A498 and 786O cells (Figure 4A-B). Subsequently, CCK8 assays were performed. After A498 and 786O cells were transfected for 5 days, the A450 OD values revealed that cells proliferation ability was significantly suppressed in RNAi1 and RNAi2 groups, and significantly promoted in OE groups compared with normal control (Figure 4C-D).

Inhibition of *FASN* increases apoptois of ccRCC cells

As shown in Figure 4E, we performed cells apoptosis detection assay in 786O cells and NC, RNAi1, RNAi2, OE groups. It suggested an increase of apoptosis cell percentage in RNAi1 and RNAi2 groups compared with 786O cells, whereas FASN overexpression showed similar apoptosis cell percentage compared with 786O cells (Figure 4F).

FASN regulates migration ability of ccRCC cells

To explore the role of FASN-mediated migration ability of ccRCC cells, we performed transwell migration assay, and found that the inhibition of *FASN* markedly restrained migrated cell numbers. Meanwhile, the overexpression of *FASN* significantly promotes migrated A498 and 786O cell counts (Figure 4G-H). Interestingly, GSEA analysis also suggested that *FASN*, together with related hub genes, significantly involved in epithelial mesenchymal transition process (NES=1.524), consistent with role of *FASN*-mediated ccRCC cells migration ability (Figure 4I).

Functional annotations and predicted signaling pathways in silico

A PPI network of FASN and its co-expression genes was established, including ACACA, ACACB, ACLY, AASDHPPT, ACSL1, ACSL3, CDC5L, MCAT, OLAH and SREBF1 (Figure 5A). As shown in Figure 5B, bubble chart illustrated the functional enrichment of 11 related genes. Significant genes involved in fatty acid biosynthetic process, fatty acid metabolic process, carboxylic acid, organic acid and lipid biosynthetic process, markedly participated in carboxylic acid binding, vitamin binding. After normalization of 11 hub genes transcriptional data, clustering analysis and heat map were displayed (Figure 5C). Functional annotations using ClueGO showed that changes in *FASN* biological processes were closely related to fatty acid biosynthesis, fatty acid biosynthetic process and fatty acid synthase activity (Figure 5D).

Significant genes and pathways obtained by GSEA

A total of 100 significant genes were obtained from GSEA, the genes with positive and negative correlation were plotted. The results illustrated that the most significant pathways including E2F targets, down-regulation of Kras signaling, estrogen response and G2M checkpoint (Figure 6A-F). Besides, the heat map shows the transcriptional expression profiles of 100 most significant up- or down-regulated genes (Figure 6G).

Discussion

In this study, we investigated whether FASN mRNA expression has a potentially implications, and its association with abdominal adipose distribution on ccRCC patients. To clarify the effect of high FASN mRNA expression on ccRCC, we examined differential FASN expression between tumor and normal para-cancerous tissues and identified prognostic value of FASN expression in FUSCC and TCGA cohorts. Then,

we detected anthropometric measures of adipose distribution on MRI. Our results showed that FASN mRNA significantly associated with elevated VAT%, and more importantly, patients with up-regulated FASN mRNA were exposed to poor PFS and OS. Additionally, after transfection efficiency was verified, we found transient inhibition and overexpression of FASN significantly regulates cells proliferation and migration abilities, and inhibition of FASN displayed higher apoptotic rate in ccRCC cells.

The correlation between adipose-related genes and tumors has become a topic of new interest, and several previous studies deeply illustrated the role of some related genes in tumorigenesis and prognostic value. Epidemiological studies in America showed that there is a significant correlation between obesity and increased incidence of cancer, and approximately 14% and 20% of cancer-related deaths are the outcome of overweight and obese, respectively [26]. Likewise, Goodwin et al. indicated that overweight and obese patients with cancer represented more aggression and worse outcomes[27]. Obesity led to over-activation of macrophages in adipose tissue and upregulation of carcinogenic compounds by changing the signal transmission between adipocytes and other cells [28]. More importantly, FASN is involved in the process of lipid metabolism and is highly expressed in tumor cells, suggesting that the high expression of FASN closely related to the occurrence and development of tumor [8]. Interestingly, after the inhibition of FASN, the proliferation of tumor cells decreased due to the decline of endogenous fatty acid synthesis, which induces cell-cycle arrest and apoptosis [29–31].

The high expression of FASN is closely related to obesity and tumor metabolism. Several studies suggested that FASN-mediated de novo synthesis of lipids may be a reasonable therapeutic target for the treatment of cancer and obesity [32]. Increased FASN is also closely associated with VAT, which owns many clinical values, such as predicting atherosclerosis [33, 34]. Importantly, atherosclerosis is inverse associated with some cancers [35], which plausibly explained the role of FASN in tumorigenesis and metastasis.

Compared with the traditional predictor BMI, we demonstrated that VAT% is a more accurate risk indicator of obesity related to ccRCC. Although BMI has been nationally accepted to be the risk factor of obesity, it has been challenged due to its rough estimation, including region, ethnic diversity and failing to distinguish fat distribution[17–19]. However, several previous studies shown that elevated VAT% is a potential cause of obesity-related carcinogenesis, which is included in colorectal adenomas [36], esophageal adenocarcinoma [37], prostate cancer [38, 39]. Our previous studies also demonstrated that VAT associated with poor prognosis and high Fuhrman grade of RCC [23, 40], and VAT seems to be more representative than BMI in predicting the prognosis of RCC.

In our institution, MRI was utilized to measure SAT as a preoperative examination for RCC patients, and VAT% was calculated after then. Although computed tomography (CT) is considered to be the standard imaging method for measuring abdominal obesity, MRI has the advantages of high accuracy and safety in measuring abdominal obesity [41–43]. The thickness of abdominal obesity varies at different levels, and in order to reduce the deviation caused by the measurement method, we measured the thickness of abdominal obesity at the level of the umbilicus.

The advantage of our study is that we first detected the expression level of FASN mRNA in ccRCC tumor and para-cancerous tissues based on two cohorts. In addition, we also proved that ccRCC patients with elevated FASN mRNA expression respond to poor PFS and OS, which was consistent with previous studies [5]. Next, we attempt to investigate the correlation between FASN and abdominal obesity distribution, especially with VAT%, which serves as a more representative indicator than BMI in investigating the individual adipose distribution for ccRCC patients. Our results showed that expression of FASN mRNA was significantly associated with abdominal adipose distribution, especially positively correlated with increased VAT%. Besides, we first performed functional annotations experiments of FASN and its involved signal hallmarks in vitro or in silico of ccRCC.

However, this study also has some limitations. First, our study failed to clarify the underlying mechanism of FASN involved in cellular lipid metabolism of ccRCC. Second, abdominal obesity distribution was measured by MRI and VAT% was directly calculated in this study. This measurement method may cause some bias and incur additional costs for patients, while only 117 patients have undergone MRI scans. Another limitation in this study is that generalizability and population variety may not conclusive enough to firmly support our results based on 913 ccRCC patients from FUSCC and TCGA cohorts.

Conclusion

In conclusion, this study demonstrated that FASN mRNA expression is positively related with aggressive proliferation, migration and predicts prognosis of ccRCC. In addition, we first reveal that elevated FASN mRNA expression is significantly correlated with abdominal obesity distribution, especially VAT%, which also is a significant predictor of poor prognosis in patients with ccRCC.

Abbreviations

PFS, progression-free survival; OS: overall survival; FUSCC, Fudan University Shanghai Cancer Center; SAT, subcutaneous adipose tissue; VAT, visceral adipose tissue; HR: hazard ratio; CI: confidence interval; MRI, magnetic resonance imaging; BMI, body mass index; ISUP, International Society of Urological Pathology; AJCC, American Joint Committee on Cancer; PPI , protein-protein interaction; GSEA, gene set enrichment analysis

Declarations

Consent for publication

Not applicable.

Availability of supporting data

The datasets used and/or analyzed during the current study are available from the corresponding author on reasonable request or online database.

Competing interests

The authors declare no potential conflicts of interest.

Funding

This study was supported by This work is supported by Grants from the National Key Research and Development Program of China (No. 2019YFC1316000), National Natural Science Foundation of China (No. 81802525).

Authors' contributions

DWY, HL Z and YY Q defined the study, discussed analyses, reference collection, interpretation, and presentation. WH X, AA and HK W draft the manuscript, developed the algorithm and interpreted the results. WH X and AA performed the RT-qPCR analysis and integrated clinicopathological data from TCGA and FUSCC cohorts. JW, WK Z and HK W performed and analyzed the in vitro experiments. WH X, XT and FN W performed bioinformatics and statistical analysis. CG M, DL C and GH S provided the experimental tools and analyzed the experiments. DW Y and HL Z reviewed the manuscript. All authors read and approved the final manuscript.

Acknowledgements

We are grateful to all patients for their dedicated participation in the current study.

Ethical Approval and Consent to participate

All of the study designs and test procedures were performed in accordance with the Helsinki Declaration II. The Ethics approval and participation consent of this study was approved and agreed by the ethics committee of Fudan University Shanghai Cancer Center (Shanghai, China). All cell lines have been tested and authenticated.

References

1. RL, S., M. KD, and J. A, *Cancer statistics, 2019.* CA: a cancer journal for clinicians, 2019. **69**(1): p. 7-34.
2. JR, S., et al., *The International Society of Urological Pathology (ISUP) Vancouver Classification of Renal Neoplasia.* The American journal of surgical pathology, 2013. **37**(10): p. 1469-89.
3. BC, L., et al., *Histological subtype is an independent predictor of outcome for patients with renal cell carcinoma.* The Journal of urology, 2010. **183**(4): p. 1309-15.
4. JC, C., et al., *Comparisons of outcome and prognostic features among histologic subtypes of renal cell carcinoma.* The American journal of surgical pathology, 2003. **27**(5): p. 612-24.

5. A, H., et al., *Fatty acid synthase over expression is an indicator of tumor aggressiveness and poor prognosis in renal cell carcinoma.* The Journal of urology, 2008. **180**(3): p. 1137-40.
6. L, W., et al., *Fatty-acid biosynthesis in man, a pathway of minor importance. Purification, optimal assay conditions, and organ distribution of fatty-acid synthase.* Biological chemistry Hoppe-Seyler, 1986. **367**(9): p. 905-12.
7. S, W., et al., *Hormonal regulation and cellular localization of fatty acid synthase in human fetal lung.* The American journal of physiology, 1999. **277**(2): p. L381-90.
8. JA, M. and L. R, *Fatty acid synthase and the lipogenic phenotype in cancer pathogenesis.* Nature reviews. Cancer, 2007. **7**(10): p. 763-77.
9. S, O., et al., *Cohort study of fatty acid synthase expression and patient survival in colon cancer.* Journal of clinical oncology : official journal of the American Society of Clinical Oncology, 2008. **26**(35): p. 5713-20.
10. AA, H., et al., *An epidemiologic and genomic investigation into the obesity paradox in renal cell carcinoma.* Journal of the National Cancer Institute, 2013. **105**(24): p. 1862-70.
11. Y, C., et al., *Body mass index and survival in patients with renal cell carcinoma: a clinical-based cohort and meta-analysis.* International journal of cancer, 2013. **132**(3): p. 625-34.
12. AG, R., et al., *Body-mass index and incidence of cancer: a systematic review and meta-analysis of prospective observational studies.* Lancet (London, England), 2008. **371**(9612): p. 569-78.
13. P, M., et al., *Body mass index trends and role of obesity in predicting outcome after radical prostatectomy.* Urology, 2008. **72**(5): p. 1106-10.
14. L, A., et al., *Body Mass Index and Metastatic Renal Cell Carcinoma: Clinical and Biological Correlations.* Journal of clinical oncology : official journal of the American Society of Clinical Oncology, 2016. **34**(30): p. 3655-3663.
15. U, D.G., et al., *Association of Systemic Inflammation Index and Body Mass Index with Survival in Patients with Renal Cell Cancer Treated with Nivolumab.* Clinical cancer research : an official journal of the American Association for Cancer Research, 2019. **25**(13): p. 3839-3846.
16. B, L.-S., et al., *Body Fatness and Cancer--Viewpoint of the IARC Working Group.* The New England journal of medicine, 2016. **375**(8): p. 794-8.
17. AJ, T., et al., *Misclassification of cardiometabolic health when using body mass index categories in NHANES 2005-2012.* International journal of obesity (2005), 2016. **40**(5): p. 883-6.
18. MD, P., et al., *Obesity misclassification and the metabolic syndrome in adults with functional mobility impairments: Nutrition Examination Survey 2003-2006.* Preventive medicine, 2014. **60**: p. 71-6.
19. EL, T., et al., *Excess body fat in obese and normal-weight subjects.* Nutrition research reviews, 2012. **25**(1): p. 150-61.
20. B, L., et al., *Correlation of fat distribution in whole body MRI with generally used anthropometric data.* Investigative radiology, 2009. **44**(11): p. 712-9.

21. KA, B., et al., *Body fat distribution, incident cardiovascular disease, cancer, and all-cause mortality.* Journal of the American College of Cardiology, 2013. **62**(10): p. 921-5.
22. MM, I., *Subcutaneous and visceral adipose tissue: structural and functional differences.* Obesity reviews : an official journal of the International Association for the Study of Obesity, 2010. **11**(1): p. 11-8.
23. WH, X., et al., *Elevated CD36 expression correlates with increased visceral adipose tissue and predicts poor prognosis in ccRCC patients.* Journal of Cancer, 2019. **10**(19): p. 4522-4531.
24. Y, Z., et al., *Visceral obesity and risk of high grade disease in clinical t1a renal cell carcinoma.* The Journal of urology, 2013. **189**(2): p. 447-53.
25. Xu, W.H., et al., *Elevated CD36 expression correlates with increased visceral adipose tissue and predicts poor prognosis in ccRCC patients.* J Cancer, 2019. **10**(19): p. 4522-4531.
26. EE, C., et al., *Overweight, obesity, and mortality from cancer in a prospectively studied cohort of U.S. adults.* The New England journal of medicine, 2003. **348**(17): p. 1625-38.
27. PJ, G. and S. V, *Impact of the obesity epidemic on cancer.* Annual review of medicine, 2015. **66**: p. 281-96.
28. C, W. and S. NL, *Obesity and tumor growth: inflammation, immunity, and the role of a ketogenic diet.* Current opinion in clinical nutrition and metabolic care, 2016. **19**(4): p. 294-9.
29. JA, M. and L. R, *Fatty acid synthase-catalyzed de novo fatty acid biosynthesis: from anabolic-energy-storage pathway in normal tissues to jack-of-all-trades in cancer cells.* Archivum immunologiae et therapiae experimentalis, 2004. **52**(6): p. 414-26.
30. JA, M. and L. R, *Oncogenic properties of the endogenous fatty acid metabolism: molecular pathology of fatty acid synthase in cancer cells.* Current opinion in clinical nutrition and metabolic care, 2006. **9**(4): p. 346-57.
31. FP, K., *Fatty acid synthase and cancer: new application of an old pathway.* Cancer research, 2006. **66**(12): p. 5977-80.
32. HP, L., et al., *Destabilization of Fatty Acid Synthase by Acetylation Inhibits De Novo Lipogenesis and Tumor Cell Growth.* Cancer research, 2016. **76**(23): p. 6924-6936.
33. R, B., et al., *High visceral fat with low subcutaneous fat accumulation as a determinant of atherosclerosis in patients with type 2 diabetes.* Cardiovascular diabetology, 2015. **14**: p. 136.
34. S, H., K. Y, and K. K, *Visceral-to-subcutaneous fat ratio is independently related to small and large cerebrovascular lesions even in healthy subjects.* Atherosclerosis, 2017. **259**: p. 41-45.
35. J, B., et al., *Comprehensive analysis of clinico-pathological data reveals heterogeneous relations between atherosclerosis and cancer.* Journal of clinical pathology, 2014. **67**(6): p. 482-90.
36. N, K., et al., *Visceral adiposity and colorectal adenomas: dose-response meta-analysis of observational studies.* Annals of oncology : official journal of the European Society for Medical Oncology, 2015. **26**(6): p. 1101-9.

37. R, M., et al., *Visceral adipose tissue: the link with esophageal adenocarcinoma.* Scandinavian journal of gastroenterology, 2014. **49**(4): p. 449-57.
38. K, O., E. F, and H. K, *Abdominal obesity, hypertension, antihypertensive medication use and biochemical recurrence of prostate cancer after radical prostatectomy.* European journal of cancer (Oxford, England : 1990), 2015. **51**(5): p. 604-9.
39. YY, Q., et al., *Influence of obesity on localized prostate cancer patients treated with radical prostatectomy.* Asian journal of andrology, 2013. **15**(6): p. 747-52.
40. HK, W., et al., *Visceral fat accumulation is associated with different pathological subtypes of renal cell carcinoma (RCC): a multicentre study in China.* BJU international, 2014. **114**(4): p. 496-502.
41. BJ, K., et al., *Comparison of 3 T MRI and CT for the measurement of visceral and subcutaneous adipose tissue in humans.* The British journal of radiology, 2012. **85**(1018): p. e826-30.
42. A, S., et al., *Predictive accuracy of single- and multi-slice MRI for the estimation of total visceral adipose tissue in overweight to severely obese patients.* NMR in biomedicine, 2015. **28**(5): p. 583-90.
43. AH, P., et al., *Adipose tissue MRI for quantitative measurement of central obesity.* Journal of magnetic resonance imaging : JMRI, 2013. **37**(3): p. 707-16.

Figures

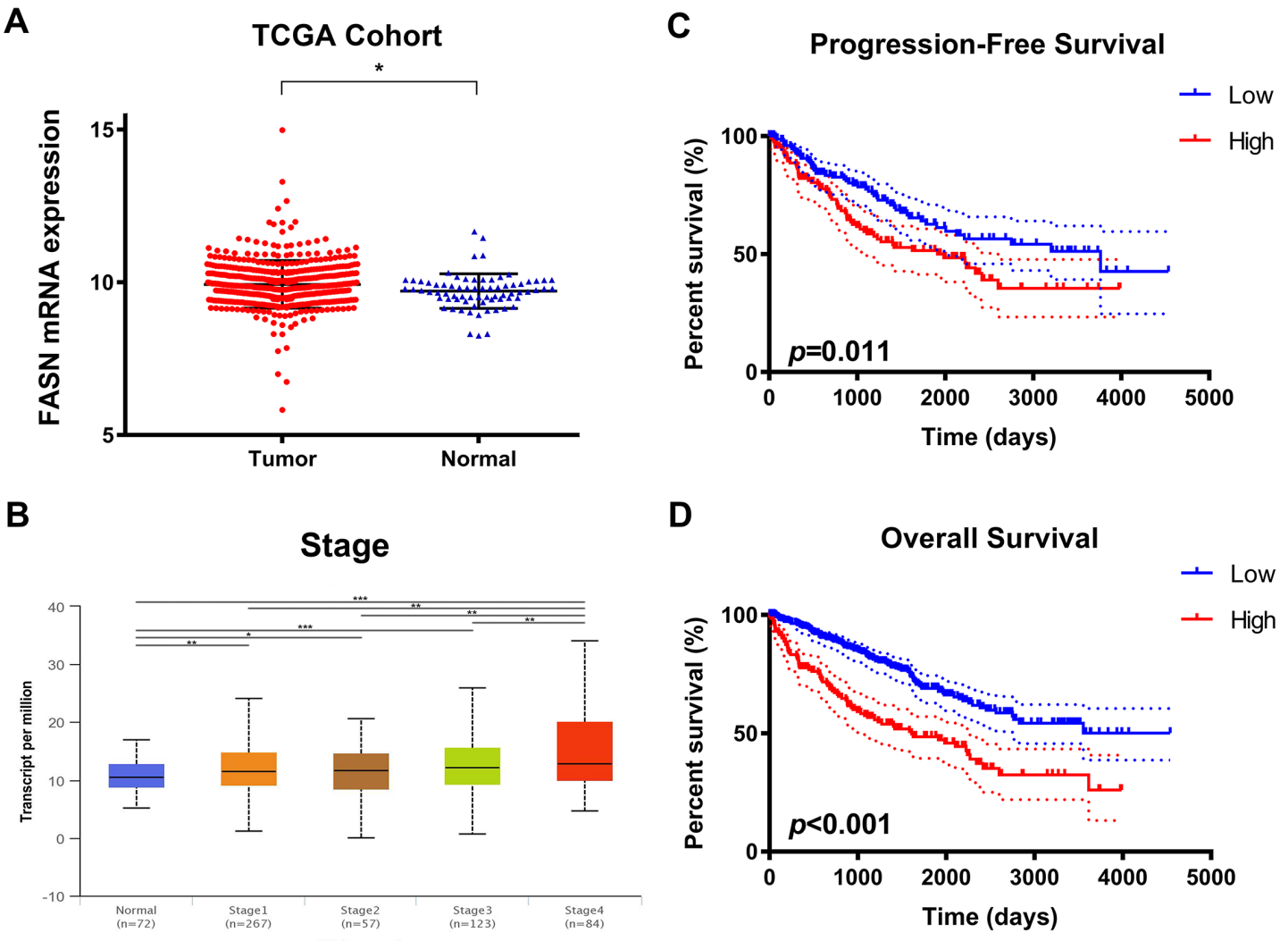

Figure 1

Differential FASN mRNA expression and its correlation with advanced clinicopathological parameters in 533 ccRCC patients from TCGA cohort. (A) Transcriptional level of FASN expression highly expressed in 533 ccRCC tissues compared with 72 normal tissues in TCGA cohort ($p<0.05$). (B) The FASN mRNA expression was markedly related with advanced clinical AJCC stage ($p<0.05$), and reached the highest in stage 4. (C-D) Survival analysis in Kaplan–Meier method indicated that elevated FASN expression was significantly associated with shorter PFS ($p=0.011$) and OS ($p <0.001$) in TCGA cohort.

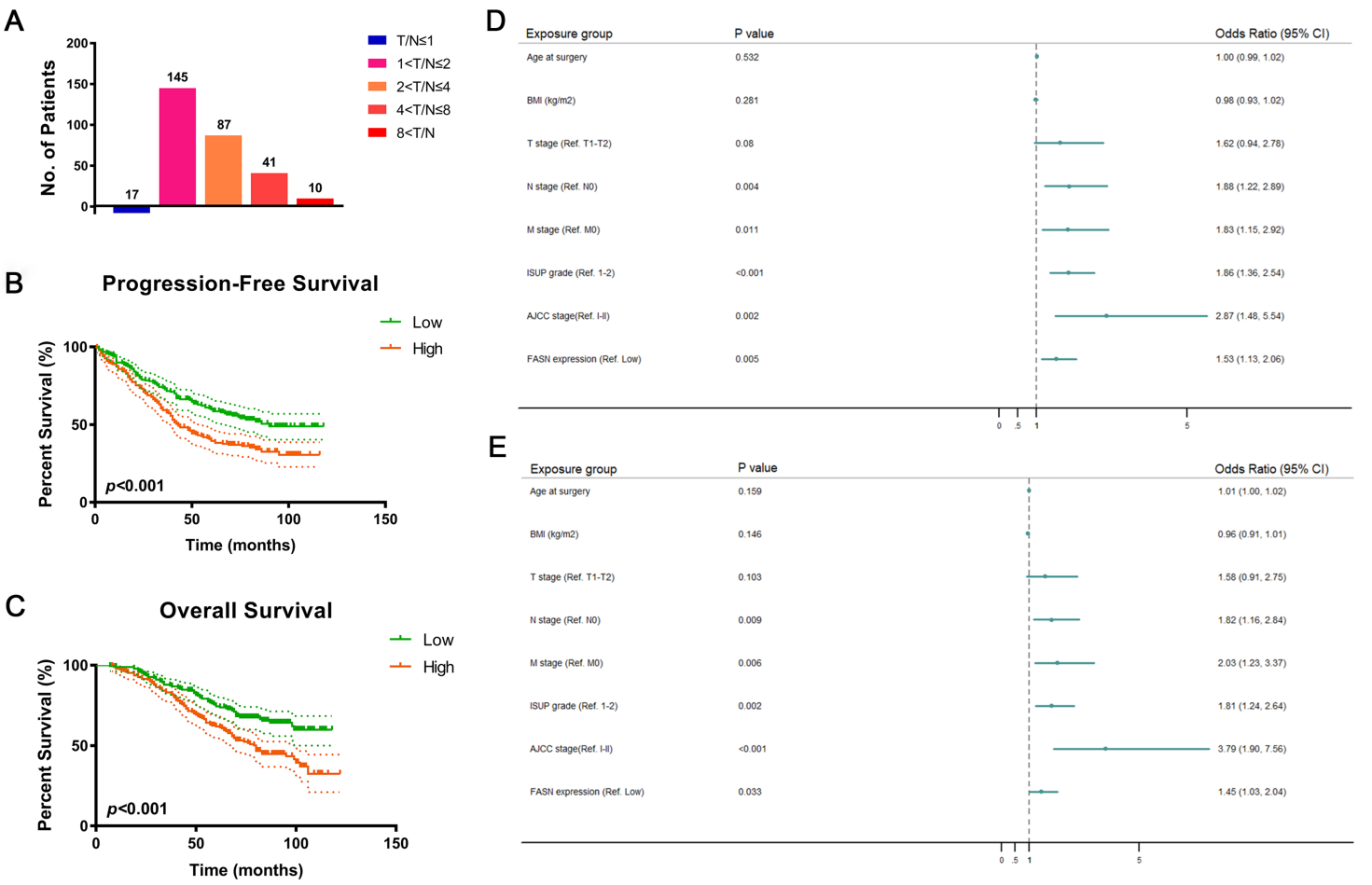

Figure 4

FASN mRNA expression and prognostic implication in 380 ccRCC patients from FUSCC cohort. (A) In order to validate FASN mRNA expression levels in ccRCC tissues in vitro, we performed Real-time qPCR on 380 pairs of ccRCC and normal samples from FUSCC cohort. The result showed that the ratio of T/N was dramatically different among the distinct of FASN mRNA expression group. (B-C) Survival analysis demonstrated that patients with higher FASN mRNA expression exhibited significantly poor PFS (p<0.001) and OS (p<0.001). (D-E) Forest plot showed multivariate Cox regression analyses of PFS and OS in 380 enrolled ccRCC patients from FUSCC cohort.

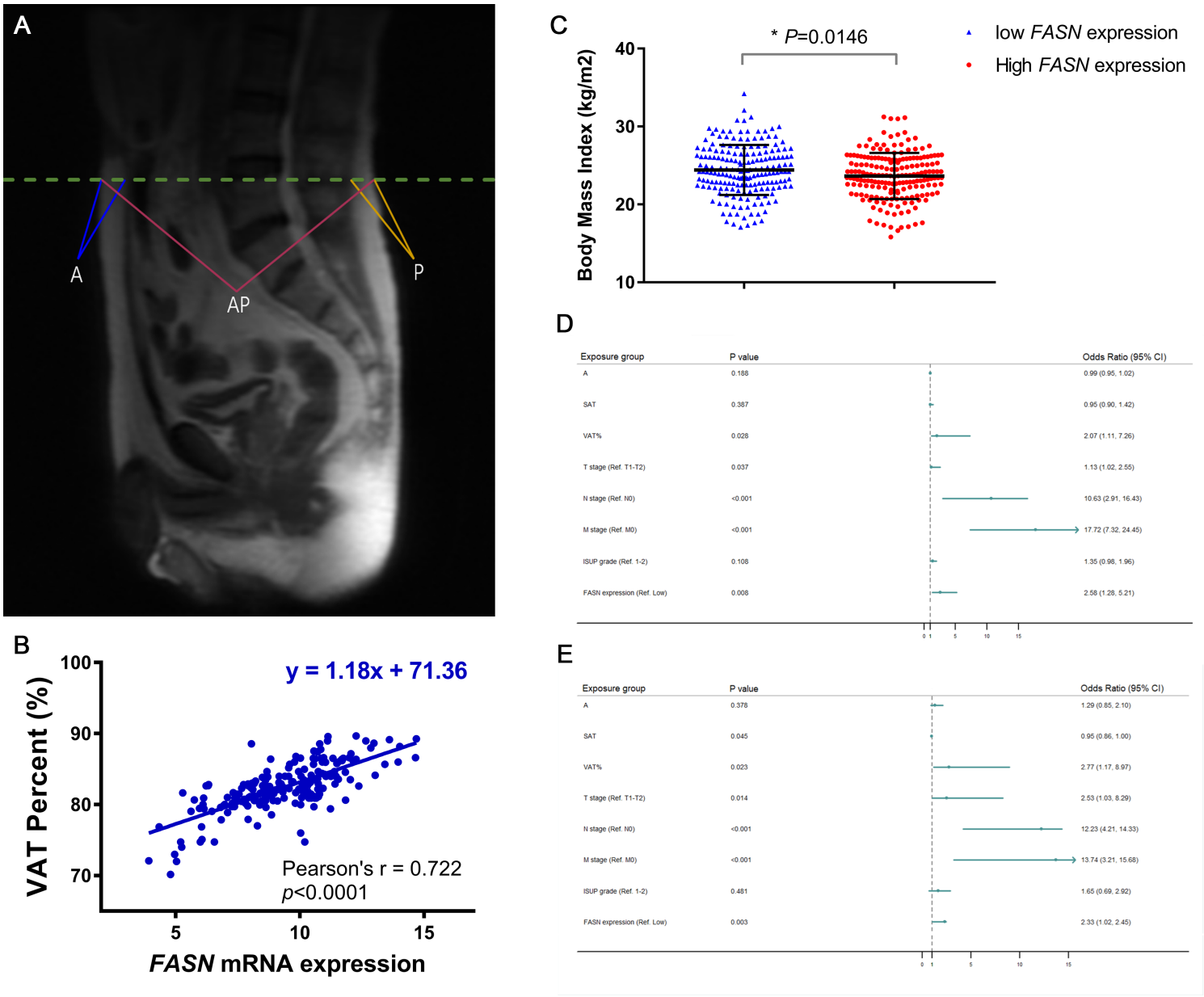

Figure 6

Anthropometric measurement of abdominal adipose and prognostic implication of VAT%. (A) The quantity of anthropometric measures of SAT area was measured by MRI with T2-weighted sagittal localization images. (B) Pearson's correlation coefficient demonstrated that elevated FASN mRNA expression was positively correlated with the VAT% (r=0.722, p<0.0001). (C) BMI in ccRCC patients with low FASN expression is higher than that in patients with high expression of FASN. (D-E) Forest plot showed multivariate Cox regression analyses of PFS and OS in 117 ccRCC cases whose MRI scans were available from FUSCC cohort.

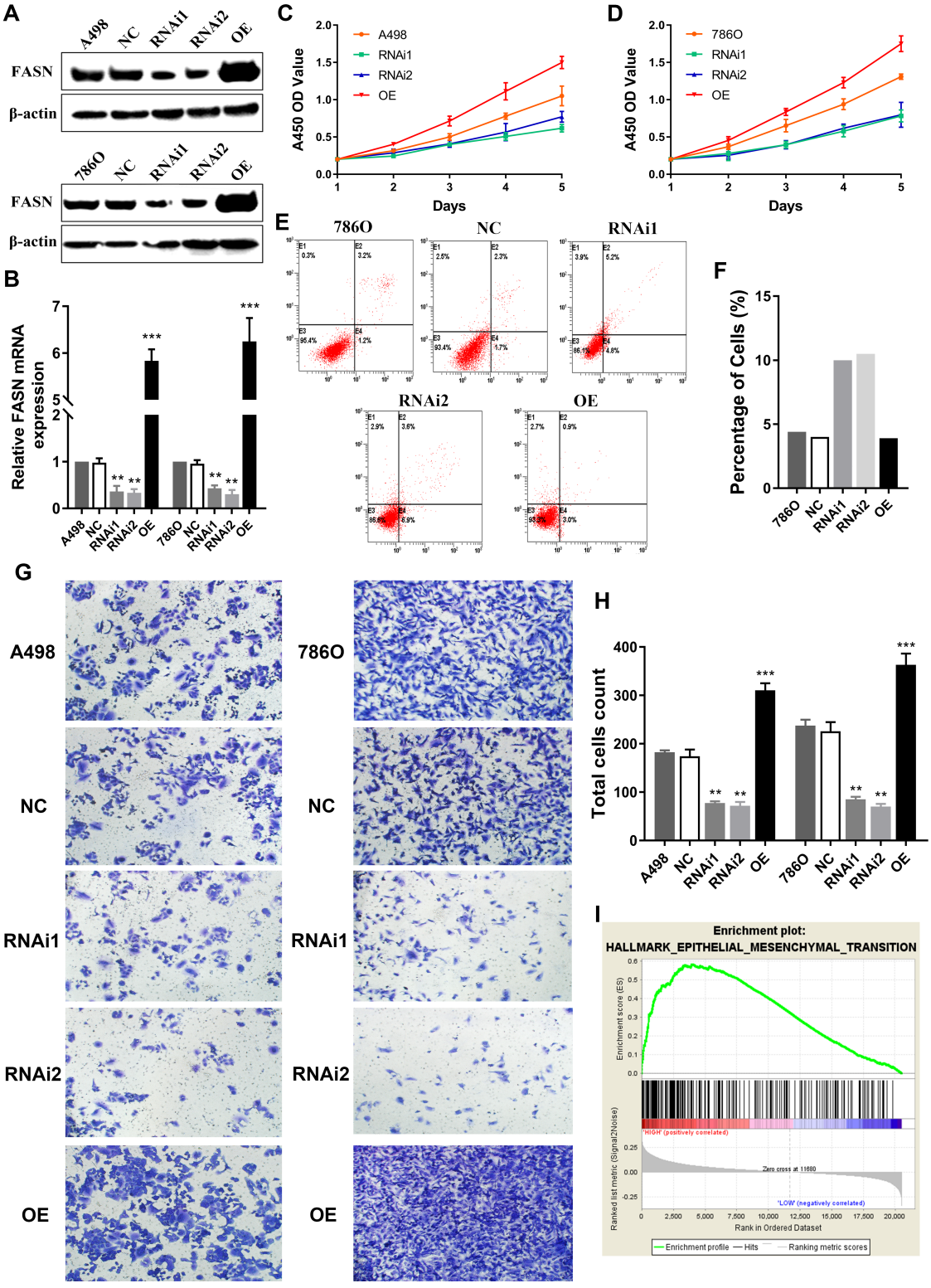

Figure 7

FASN regulates proliferation, apoptosis and migration of human ccRCC cells. (A-B) After transient transfected with FASN plasmid in normal control, FASN-RNAi1, FASN-RNAi2 and FASN-overexpression (OE) groups, we investigated FASN mRNA and protein expression level in A498 and 786O cells, and found significant differential expression levels in RNAi1, RNAi2 and OE groups compared with A498 and 786O cells. (C-D) After A498 and 786O cells were transfected for 5 days, the A450 OD values revealed that cells

proliferation ability was significantly suppressed in RNAi1 and RNAi2 groups, and significantly promoted in OE groups compared with normal control. (E-F) We performed cells apoptosis detection assay in 786O cells and NC, RNAi1, RNAi2, OE groups. It suggested an increase of apoptosis cell percentage in RNAi1 and RNAi2 groups compared with 786O cells, whereas FASN overexpression showed similar apoptosis cell percentage compared with 786O cells. (G-H) To explore the role of FASN-mediated migration ability of ccRCC cells, we performed Transwell migration assay, and found that the inhibition of FASN markedly restrained migrated cell numbers. Meanwhile, the overexpression of FASN significantly promotes migrated A498 and 786O cell counts. (I) GSEA analysis also suggested that FASN, together with related hub genes, significantly involved in epithelial mesenchymal transition process (NES=1.524).

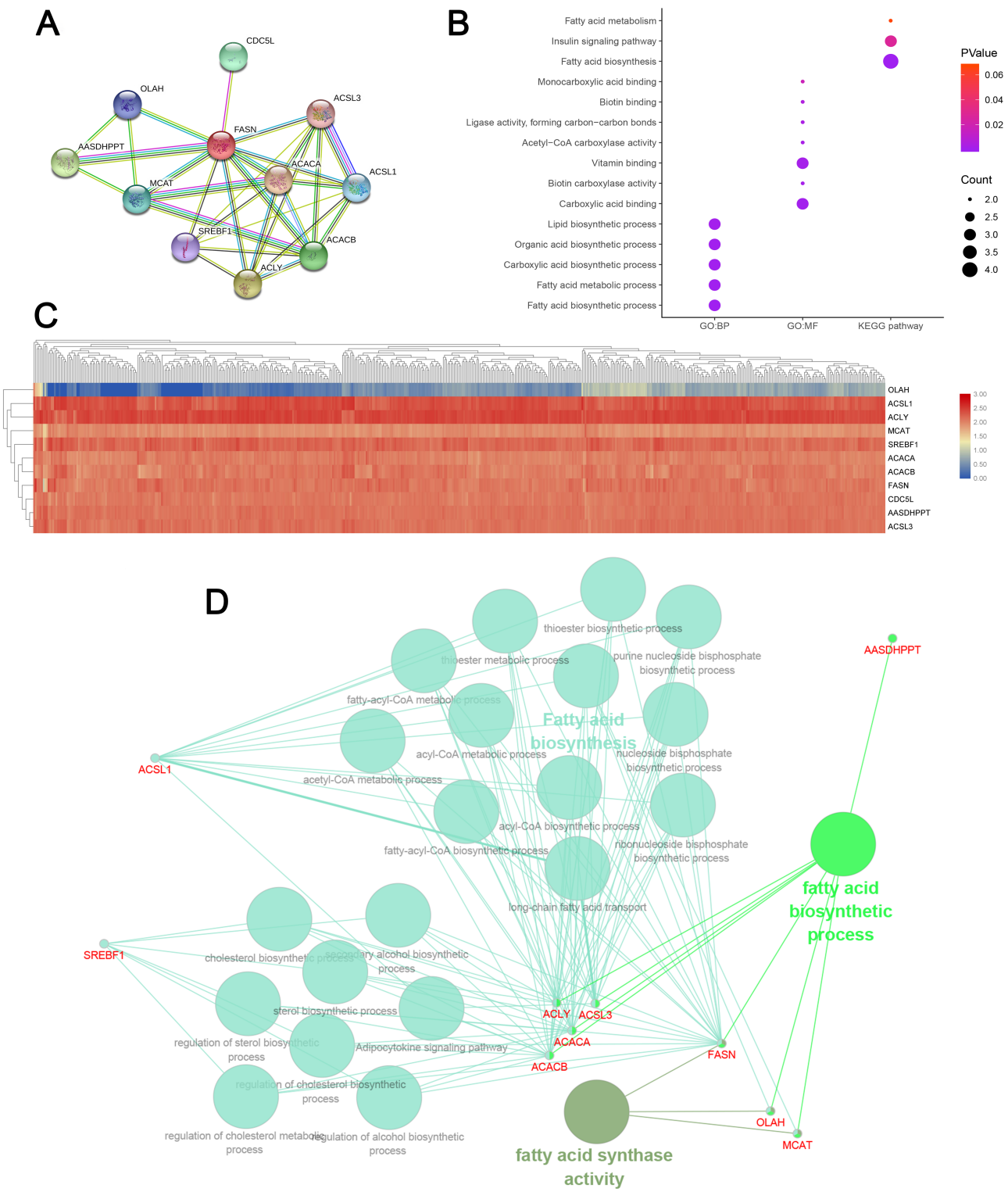

Figure 10

Functional annotations and predicted signaling pathways in silico. (A) A PPI network of FASN and its co-expression genes was established, including ACACA, ACACB, ACLY, AASDHPPT, ACSL1, ACSL3, CDC5L, MCAT, OLAH and SREBF1. (B) Functional enrichment analyses of a total of 11 involved genes were performed and visualized in bubble chart. Significant genes involved in fatty acid biosynthetic process, fatty acid metabolic process, carboxylic acid, organic acid and lipid biosynthetic process, markedly

participated in carboxylic acid binding, vitamin binding. (C) Horizontal and vertical cluster analysis was performed in 533 ccRCC samples from TCGA database and 11 related genes, and the heat map was obtained after standardization. (D) Functional annotation using ClueGO indicated that changes in the biological processes of the FASN were significantly associated with fatty acid biosynthesis, fatty acid biosynthetic process and fatty acid synthase activity.

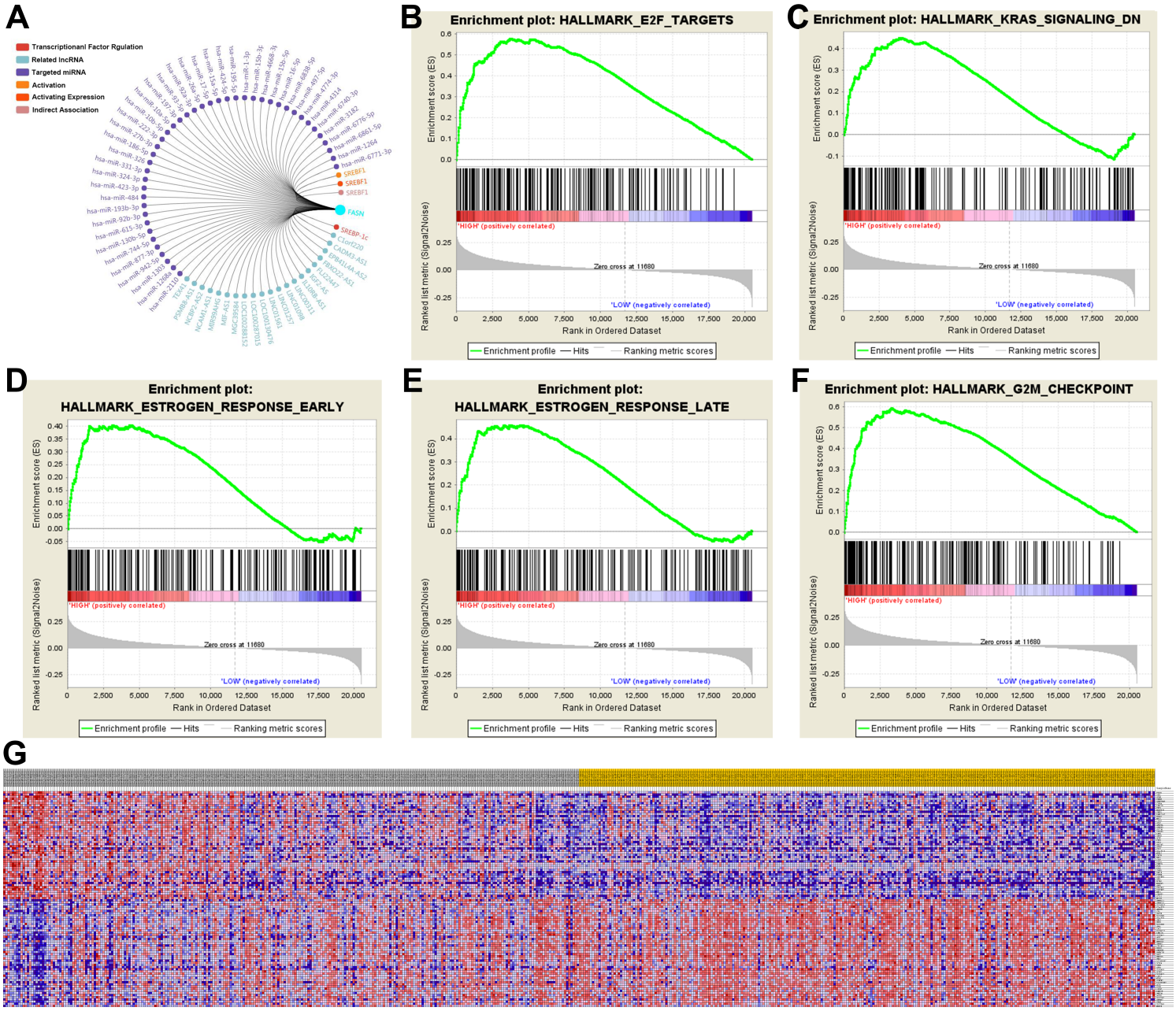

Figure 12

Significant related genes and hallmarks pathways in ccRCC obtained by GSEA. (A-F) The most significant pathways include E2F targets, down-regulation of Kras signaling, estrogen response and G2M checkpoint. (G) Transcriptional expression profiles of a total of 100 significant genes with positive and negative correlation were performed in a heat map.

Supplementary Files

This is a list of supplementary files associated with this preprint. Click to download.

- supplementary.docx
- supplementary.docx